http://dx.doi.org/10.15576/GLL/2023.4.41

GLL

Geomatics, Landmanagement and Landscape No. 4 • 2023, 41–57

GEOSPATIAL MODELING FOR ENHANCED LANDSLIDE SUSCEPTIBILITY MAPPING IN ATLAS MOUNTAINS OF THE NORTHEAST OF ALGERIA

Rania Boudjellal, Chemseddine Fehdi, Fethi Baali

Summary

This study presents a practical geospatial approach, based on geomatic principles, to create landslide susceptibility maps that meet contemporary landscape and land management priorities. By employing a GIS-based statistical modeling, our methodology seamlessly integrates a wide range of factors including topography, lithology, land use, and precipitation. This comprehensive approach allows for a holistic evaluation of landslide susceptibility. We use two widely recognized multi-criteria techniques, namely the Analytic Hierarchy Process (AHP) and the Fuzzy Logic Ratio (FR), which in result produce two distinct yet complementary landslide susceptibility maps (LSMs). The creation of these LSMs relies on a carefully curated dataset of landslides, collected through rigorous analysis of high-resolution satellite imagery, interpretation of aerial photographs, and extensive fieldwork. Eleven key factors are selected to inform the modeling process. To assess the accuracy of the LSMs, we employ ROC curves, with the FR method demonstrating superior predictive performance, achieving an impressive accuracy rate of 75% compared to the AHP model's 65%. These findings highlight the effectiveness of our approach in identifying high landslide susceptibility areas, providing valuable insights for informed land use planning, hazard mitigation strategies, and rapid emergency response measures. The GIS-based statistical modeling technique showcased in this research provides a robust framework for generating precise landslide susceptibility maps in complex mountainous landscapes. This research makes a significant contribution to the evolving field of geomatics, enhancing landscape resilience and promoting sustainable land management practices.

Keywords

geospatial approach • landslide susceptibility maps • GIS-based modeling • multi-criteria analysis • landscape resilience

1. Introduction

The Mediterranean region is susceptible to a wide range of natural hazards, each of which posies significant risks that can cause extensive damage and loss of life. Landslides, earthquakes, and floods are particularly noteworthy among these threats, as each presents distinct challenges and consequences. These catastrophic events are capable of wreaking havoc on the affected areas that leaves a trail of devastation [Sánchez-García and Mateos, 2020]. These challenges impede progress and undermine efforts to promote sustainable, long-term development in the region [Manchar et al. 2018, Brahmi et al. 2021, Bagwan et al. 2023, Sankar et al. 2023, Orabi et al. 2023a, b, Taib et al. 2023]. In recent years, Northeast Algeria has witnessed a rise in devastating landslides triggered by various factors, such as heavy rainfall, seismic activity, and human activities, including improper land use and construction practices [Dahoua et al. 2017a, b, 2018, Karim et al. 2018, Kerbati et al. 2020, Fredj et al. 2020, Nekkoub et al. 2020, Mahleb et al. 2022, El Hafyani et al. 2023, Asmoay and Mabrouk 2023].

The use of Geographic Information System (GIS) techniques has become increasingly important in the assessment of landslide susceptibility. A variety of methods have been developed, including statistical models, machine learning algorithms, and expert systems [Van Westen et al. 2003, Lee and Sambath 2006, Lee and Pradhan 2007, Raïs et al. 2017, Merghadi et al. 2020]. These models use statistical analysis to explore the relationship between landslide occurrence and the factors that control it [Neuhäuser and Terhorst 2007, Mahdadi et al. 2018, Kallel et al. 2018, Boubazine et al. 2022, Dib et al. 2022].

This study focuses on the assessment of landslide susceptibility in the Wadi Maleh and middle Seybouse sub-catchments, employing the Analytic Hierarchy Process (AHP) method introduced by Saaty [1980]. As an approach recognized by researchers worldwide, AHP has demonstrated to be effective in landslide susceptibility analysis [Achour et al. 2017]. AHP involves pairwise comparisons of decision variables, yielding relative dominance values on a scale from 1 to 9. This allows for both qualitative and quantitative assessment of priorities [Saaty 2000]. Furthermore, the study incorporates the Frequency Ratio (FR) model to assess landslide susceptibility. This model examines the ratio between areas affected by landslides and those unaffected to calculate the influence of each factor on the occurrence of landslides.

It is essential to recognize that each of these approaches operates under specific assumptions. By employing both the AHP and FR methods, this study provides a comprehensive analysis of landslide susceptibility in the study area, thus facilitating well-informed decision-making to mitigate potential impacts on both people and infrastructure.

2. Study area

Our study area, situated within the Tellian Atlas chain (Fig. 1), covers 1373 square kilometers across seven provinces in the eastern region of Algeria. This region features a diverse topography, including undulating hills and towering mountains, with elevations ranging from 100 to 1400 meters above sea level. Notable peaks in this landscape include Jebel Mahouna at 1411 meters and Ras El Alia at 1317 meters above sea level. Natural processes have shaped the terrain, resulting in distinctive landforms. The surrounding hills have gentle slopes, while their summits are gracefully rounded. The area has a semi-arid climate, characterized by cold winters with temperatures as low as 5°C and hot summers with temperatures reaching up to 40°C. Annual precipitation, reaching a maximum of 800 mm, sustains the land. A network of waterways, including Wadi Maiz, Wadi Zimba, Wadi Bousora, and Wadi Helia, contributes to the hydrology of the Guelma sub-basin. Particularly noteworthy is the Maleh sub-basin, which includes Rbiba, Sekaka, EL Hamam, Zouara, Cheham, and Ghanem wadis, converging to form the Seybouse River, the primary watercourse in the study area.

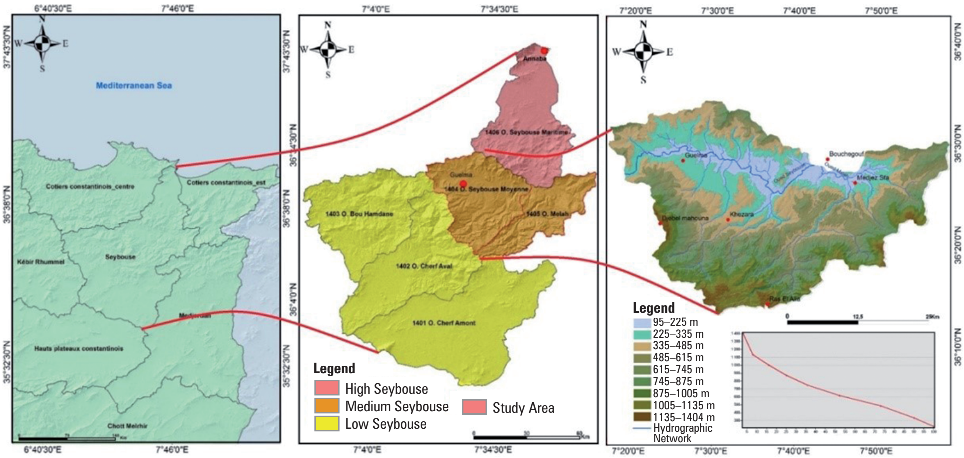

Source: Authors' own study

Fig. 1. Location map of the study area

Geologically, there is an array of rock formations dating from the Jurassic to the Quaternary period found in this region. These include carbonate deposits, Triassic diapiric extrusions of plastic clay and gypsum to the north of Hammam N'bail, and Liassic limestone formations surrounding Jebel Nador. Upper Cretaceous marl, Aptian marls, Barremian black marls with pyritic ammonites, Albian marls adorned with light micritic limestone, and Vraconian marls compose the geological mosaic of the study area. Noteworthy geological features include the presence of the Numidian thrust sheet, Tellian thrust sheet, and Ultra Tellian series, each of which has played a distinct role in the geological history. Adjacent to Jebel Debagh, the Penthièvre flysch extends towards the southeast, covering geological periods from the Cenomanian to the Oligocene. Further south, the Guerouche flysch characterizes the landscape at the eastern tip of Jebel Debagh and to the west of the Beni Mezline forest. These formations, comprising primarily sandstone strata interspersed with clay-schist intercalations, fine limestone, and clayey sandstone, define the geology of the area. The study area bears the marks of the Mio-Pliocene period, characterized by sandy clays, red conglomerates, pebbles, and fine sandstone. The Quaternary era created several alluvial terraces that include conglomerates, silt, clays, and gravel, each layer preserving a record of time (Fig. 2). These intricate geological formations, shaped over millennia, provide a rich canvas for studying the factors related to landslide susceptibility, adding a unique dimension to the study of Geomatics, Landscape, and Land Management in this region, and highlighting the complex interplay between geological heritage and the dynamic landscape.

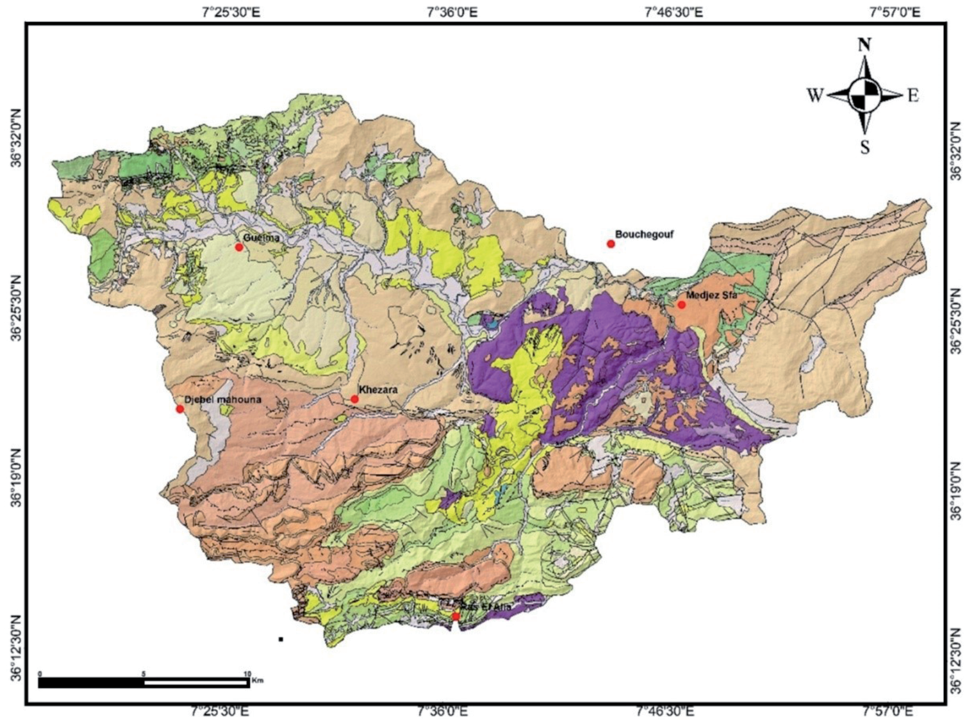

Source: Authors' own study

Fig. 2. Geological map of the study area

3. Material and methods

This research aimed to assess the likelihood of landslides in the study area using probabilistic techniques, relying on a comprehensive spatial database. Data from multiple sources, including geological maps and satellite images, were collected to create this database. The methodology involved standardizing variables, weighting factors, and grouping criteria. Statistical analysis was performed using Excel Stat Pro, and GIS processing was carried out using ArcGIS 10.8. In summary, this study established a robust spatial database for landslide susceptibility analysis, integrating various data sources and advanced analytical tools.

3.1. Landslide inventory

In our study area, we conducted extensive field surveys, aerial photo analysis, and satellite image analysis (Rapid-Eye, PS Ortho Tile) to identify and map 497 landslides. Our observations revealed higher landslide occurrence in the south and southeast regions, dominated by marl and clay formations, and lower occurrence in the northwestern region with limestone formations (Fig. 3a). These data are crucial for evaluating landslide susceptibility and developing predictive models.

3.2. Landslide-conditioning factors

3.2.1. Slope angle

The assessment of slope stability heavily relies on the slope angle, and it is commonly used in the creation of landslide susceptibility models [Saha et al. 2005]. In our study, a slope angle map of the area was generated from a digital elevation model (DEM) and subsequently reclassified into five equal classes (Fig. 3b).

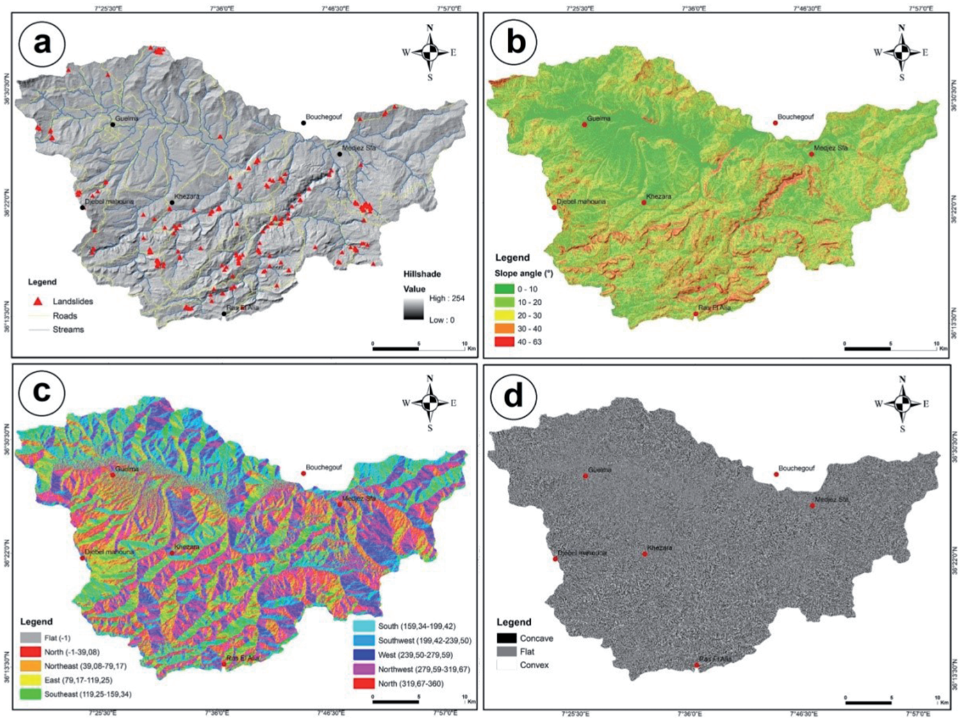

Source: Authors' own study

Fig. 3. **a.** Landslide inventory map of the study area. **b.** Slope map (in degree). **c.** Slope aspect map. **d.** Curvature plane map

3.2.2. Slope aspect

Slope aspect, which refers to the direction of the slope, is recognized as a significant factor affecting landslide occurrence [Pourghasemi et al. 2012]. In our study, the slope aspect of the area is categorized into nine directional classes (Fig. 3c).

3.2.3. Plane curvature

Plane curvature affects the convergence or divergence of water during downflow [Yilmaz et al. 2012]. In our study, the Geographic Information System in ArcGIS 10.8 was used to derive the plane curvature from the DEM. The curvature was then classified into three categories: concave, convex, and flat (Fig. 3d).

3.2.4. Elevation

Elevation is a commonly used factor in the assessment of landslide susceptibility. In our study, the study area's altitude ranged from 95 to 1404 meters above sea level. We divided the elevation values into five equal intervals of 230 meters each to facilitate analysis (Fig. 3e).

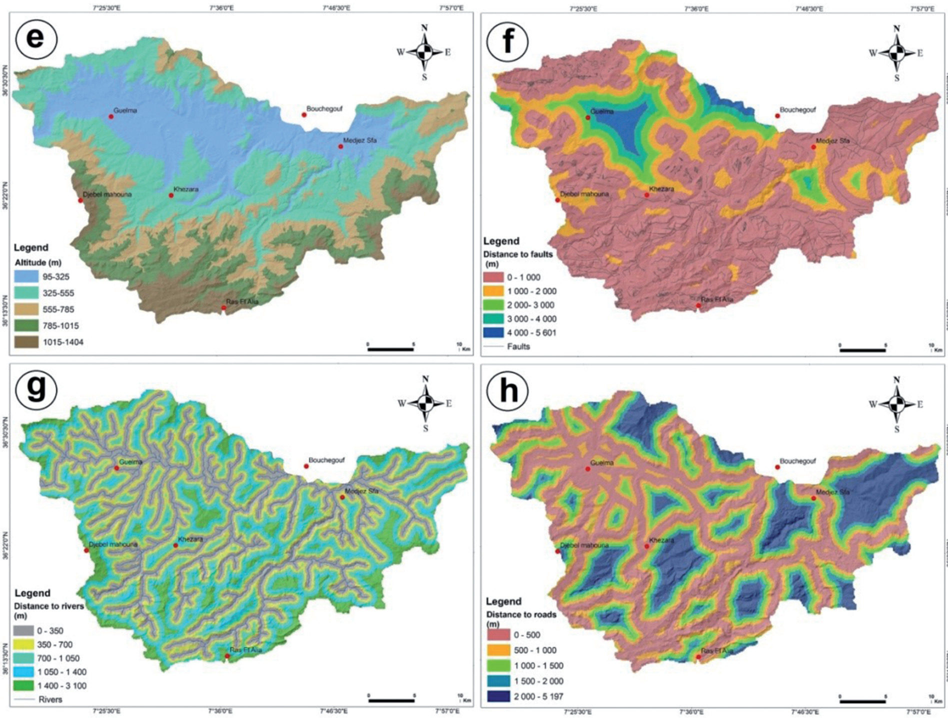

Source: Authors' own study

Fig. 3. **e.** Elevation map of the study area. **f.** Fault distance map. **g.** Map of distance to rivers. **h.** Road distance map

3.2.5. Distance to faults

Faults have the potential to trigger landslides by causing tectonic fractures that can reduce the strength of rocks [Foumelis et al. 2004]. For the purposes of our study, the faults were extracted from the 1:50,000 geological maps. The distance to the faults was determined using a buffer method, with intervals of 1000 m (Fig. 3f).

3.2.6. Distance to rivers

In mountainous regions, runoff is a key factor in triggering landslides, since rivers are the main mechanism causing them [Wang et al. 2019]. To assess the impact of watercourses on the slopes in our study area, we created five distinct buffer zone categories. These categories allowed us to examine the degree to which watercourses influenced the slopes (Fig. 3g).

3.2.7. Distance to roads

Human activity, particularly road construction, is a major contributor to landslides [Dahal et al. 2008]. The excavation of cut slopes during road construction can alter the natural topography and lead to slope instability. In our study, we aimed to examine the impact of roads on slope stability by dividing the study area into five buffer zones with 500 m intervals based on distance from the road (Fig. 3h).

3.2.8. SPI

Assessing the SPI of a particular area can help to identify regions that may be at higher risk of landslides and inform mitigation efforts. [Conforti et al. 2011]. The study area's SPI map has been divided into five distinct categories (Fig. 3i).

3.2.9. TWI

Assessing the TWI of a particular area can help to identify regions that may be at higher risk of landslides and inform mitigation efforts [Pourghasemi et al. 2013]. Five categories were used to classify the TWI values (Fig. 3j).

3.2.10. Lithology

Lithology is a factor often considered in landslide stability analysis. As mentioned earlier, the geological maps at a scale of 1:50,000 were used to generate the lithological map of the study area. The study area is characterized by a range of lithological units, which includes soft clayey as well as hard rock facies (Fig. 3h).

3.2.11. Precipitation

Rainfall intensity and duration, with short, intense bursts being more likely to trigger landslides, require close monitoring to identify high-risk regions and deliver early warnings. A precipitation isohyets map is generated by interpolating data from multiple locations, connecting points of equal precipitation levels with contour lines (Fig. 3k).

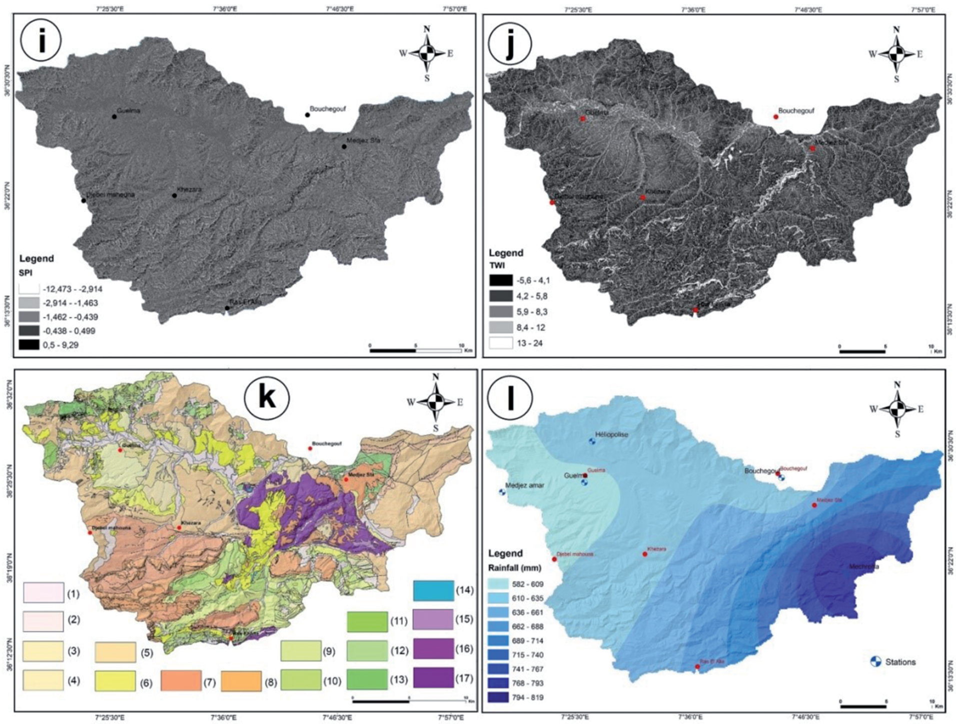

Source: Authors' own study

Fig. 3. **i.** Stream Power Index (SPI) map. **j.** Topographic Wetness Index (TWI) Map, **k.** lithologic map of the study area. **l.** rainfall map of the study area

3.3. Methodology

3.3.1. Analytical Hierarchy Process (AHP) Model

The Analytical Hierarchy Process (AHP) is a versatile decision-making tool developed by Thomas Saaty in the 1980s. It combines qualitative and quantitative approaches to assess complex problems with multiple criteria. AHP uses pairwise comparisons on a scale of 1 to 9 to rank the relative importance of factors. Decision-makers can evaluate both tangible and intangible criteria, making it adaptable to various contexts. AHP provides a decision-making structure that supports informed choices.

3.3.2. Frequency Ratio Model

The frequency ratio (FR) method assesses landslide susceptibility by analyzing past landslide events in relation to various factors. It quantifies the association between each factor and landslide events, supporting susceptibility evaluation. FR is expressed as the ratio of landslides in a class to the total number in the study area. Factors are assigned FR values, and a Landslide Susceptibility Index (LSI) is calculated by summing the FR values for each factor class. This approach helps prioritize landslide susceptibility factors.

In summary, the methodology includes AHP for weighted factor evaluation and the FR model for landslide susceptibility assessment.

4. Result and discussion

4.1. Analytical Hierarchy Process (AHP) model

In the GIS-based approach, landslide susceptibility maps were prepared using two weighting procedures based on pairwise comparisons. Table 1 presents the relative weights of the causal factors, with slope angle having the highest weight of 0.23, followed by lithology (0.20) and precipitation (0.18). These factors were integrated into a landslide susceptibility index (LSI_{Ahp}) using a weighted linear sum. The LSM_{Ahp} was generated from the LSI_{Ahp}, hierarchized into five susceptibility zones (very low, low, moderate, high, and very high), with the southern part being highly susceptible, and the center and northwest areas having low susceptibility. Approximately 41.638% of the total area is not susceptible to landslides, while moderately sensitive, high, and very highly susceptible areas make up the rest (Fig. 4a).

Table 1. Pairwise comparison matrix and corresponding factor weights in Analytical Hierarchy Process (AHP)

Influencing factors	Pair-wise comparison matrix											
	(1)	(2)	(3)	(4)	(5)	(6)	(7)	(8)	(9)	(10)	(11)	Weight
(1) Slope angle	1	2	2	3	4	6	7	7	7	6	6	0.23
(2) Lithology		1	2	3	5	5	6	6	7	7	4	0.20
(3) Precipitation			1	3	5	5	6	6	7	6	7	0.18
(4) Distance to faults				1	3	6	5	7	7	6	7	0.13
(5) Distance to roads					1	3	3	5	4	6	5	0.08
(6) Distance to rivers						1	2	3	4	4	4	0.05
(7) Slope aspect							1	3	4	4	5	0.04
(8) Altitude								1	3	3	3	0.03
(9) Curvature plane									1	3	4	0.02
(10) SPI										1	2	0.02
(11) TWI											1	0.02

4.2. Frequency Ratio (FR) Model

The FR method assessed the correlation between landslide occurrence and 11 conditioning factors by calculating FR ratios based on factor class weights (Table 2). High

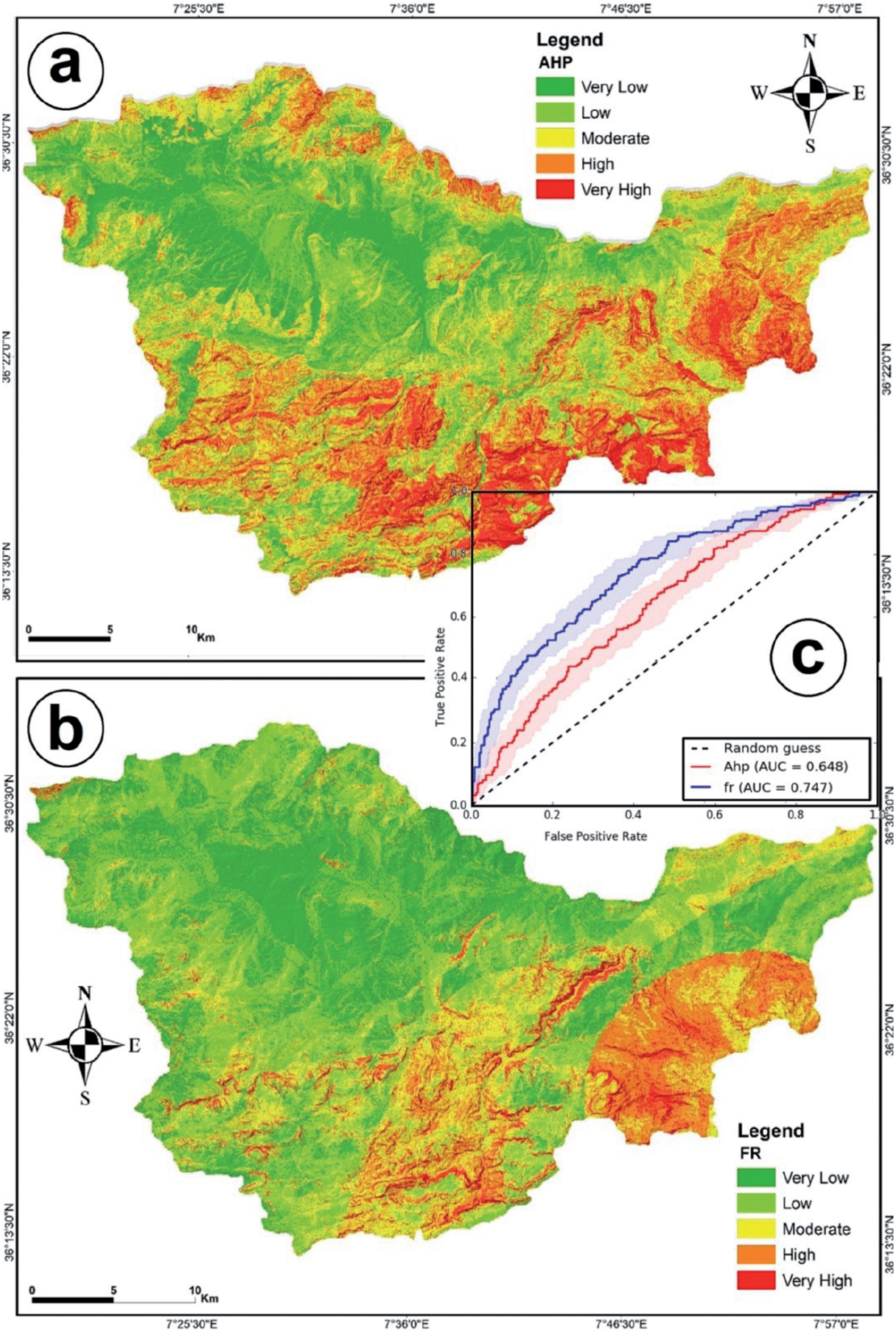

Source: Authors' own study

Fig. 4. **a.** Landslide susceptibility map derived from the AHP model. **b.** Landslide susceptibility map derived from the FR model. **c.** AUC validation of Ahp and FR models

landslide probability was observed in clay and marl formations, especially at altitudes between 555–785 m a.s.l. and precipitation levels of 750–820 mm. Close proximity to streams, faults, and roads had the greatest influence, as did concave slopes. SPI and TWI classes from −12.473 to −2.914 and 2,680.141 to 5,442.755, respectively, showed significant influence. Steep slopes (40–63 degrees) had the highest FR ratios, while flat slopes (0–10 degrees) had the lowest. The southwest aspect class had the highest FR ratio, while the east class had the lowest. The susceptibility map highlighted areas with steep slopes, Triassic facies, and high precipitation as most susceptible (Fig. 4b).

Table 2. Spatial relationship between each of the conditioning factors of landslides and the landslides by FR

N	Data layers	Class	Class pixels	% Class pixels	Landslide pixels	% Landslide pixels	FR
1	Lithology	Limestone, sandstone lim and marl-lim	518838	30.108	280	25.408	0.844
		Alluvia, scree	354903	20.595	170	15.426	0.749
		Flysch micaceous sandstone	29036	1.685	4	0.363	0.215
		Marls	360948	20.945	281	25.499	1.217
		Clays	459554	26.667	367	33.303	1.249
2	Precipitation	580–600	75117	4.354	20	1.821	0.418
		600–650	972623	56.370	196	17.851	0.317
		650–700	316183	18.325	391	35.610	1.943
		700–750	182560	10.581	37	3.370	0.318
		750–820	178929	10.370	454	41.348	3.987
3	Slope angle	0–10	470016	27.275	78	7.078	0.260
		10–20	596172	34.596	178	16.152	0.467
		20–30	406779	23.605	251	22.777	0.965
		30–40	190115	11.032	315	28.584	2.591
		40–63	60176	3.492	280	25.408	7.276
4	Altitude	95–325	446746	25.924	113	10.254	0.396
		325–555	554204	32.160	310	28.131	0.875
		555–785	342963	19.902	441	40.018	2.011
		785–1015	243701	14.142	87	7.895	0.558
		1015–1404	135644	7.871	151	13.702	1.741

Table 2. cont.

N	Data layers	Class	Class pixels	% Class pixels	Landslide pixels	% Landslide pixels	FR
5	Fault distance	0–1000	1151926	66.762	840	76.503	1.146
		1000–2000	320485	18.574	159	14.481	0.780
		2000–3000	161006	9.331	95	8.652	0.927
		3000–4000	25441	1.474	4	0.364	0.247
		4000–5601	66554	3.857	0	0	0
6	Distance to rivers	0–1000	645813	37.429	520	47.359	1.265
		1000–1500	585420	33.929	414	37.705	1.111
		1500–2000	341463	19.790	135	12.295	0.621
		2000–2500	121875	7.064	23	2.095	0.297
		2500–3093	30841	1.787	6	0.546	0.306
	Distance to roads	0–500	697874	40.447	608	55.373	1.369
		500–1000	577278	33.457	247	22.495	0.672
		1000–1500	284404	16.483	121	11.020	0.669
		1500–2000	120585	6.989	121	11.020	1.577
		2000–5197	45271	2.624	1	0.091	0.035
8	Slope aspect	North (–1–39.08)	211841	12.293	113	10.254	0.834
		Northeast (39.08–79.17)	187043	10.854	71	6.443	0.594
		East (79.17–119.25)	194989	11.315	66	5.989	0.529
		Southeast (119.25–159.34)	191674	11.123	76	6.897	0.620
		South (159.34–199.42)	188654	10.948	90	8.167	0.746
		Southwest (199.42–239.50)	161355	9.363	236	21.416	2.287
		West (239.50–279.59)	174514	10.127	173	15.699	1.550
		Northwest (279.59–319.67)	195286	11.332	142	12.886	1.137
		North (319.67–360)	217902	12.645	135	12.250	0.969
9	Curvature plane	–7.371– –0.335	354460	20.569	352	31.942	1.553
		–0.335–0.356	1010265	58.625	476	43.194	0.737
		0.356–8.648	358533	20.806	274	24.864	1.195

10	twi	–5.6–4.1	1712235	99.360	1095	99.365	1.000
		4.1–5.8	6581	0.382	0	0	0
		5.8–8.3	2615	0.152	6	0.5445	3.588
		8.3–12	1031	0.060	1	0.0907	1.517
		12–24	796	0.046	0	0	0
11	spi	–12.472– –2.914	30946	1.796	83	7.532	4.194
		–2.914– –1.463	155560	9.027	107	9.710	1.076
		–1.463– –0.439	326223	18.931	68	6.171	0.326
		–0.439–0.499	913171	52.991	383	34.755	0.656
		0.499–9.289	297358	17.256	461	41.833	2.424

4.3. Validation and comparison of results

Two different models were used to create the landslide susceptibility maps, and their results were compared to existing landslide data. 70% of the inventoried landslides were randomly chosen as training data, with the remaining 30% were used for validation. The area under the curve method assessed model predictability, with the AUC values calculated through rate curves. The model with the highest AUC was considered the best. AHP and FR models had AUC values and training accuracies of 0.648/64.80% and 0.747/74.70%, respectively (Fig. 4c). Both models demonstrated reasonable prediction accuracy for spatial landslide hazard analysis, but the FR model produced the superior landslide sensitivity map in the study area.

5. Conclusions, recommendations and outlook perspectives

In conclusion, this study has contributed to a better understanding of landslide susceptibility in the Wadi Mellah and Middle Seybouse sub-basins of northeast Algeria. The application of GIS-based techniques, specifically the Analytic Hierarchy Process (AHP) and Frequency Ratio (FR) models, allowed for a comprehensive assessment of landslide susceptibility. Eleven key factors were considered in the analysis, providing a holistic view of the terrain's susceptibility to landslides. The identification and mapping of 497 landslides, followed by model generation and validation, resulted in the creation of landslide susceptibility maps that categorized the study area into five sensitivity classes. Notably, these maps identify areas of high susceptibility in the south and southeast regions, indicating the need for targeted risk mitigation efforts.

Validation outcomes demonstrated that the FR model outperformed the AHP model in terms of accuracy, with the former achieving an accuracy rate of 74.70% compared 64.80% for the latter. This highlights the importance of employing multiple models to enhance the accuracy of landslide prediction and mapping, thereby assisting decision-makers in effectively managing landslide-related risks.

Recommendations

Continued Monitoring: Regular monitoring of the study area's susceptibility to landslides is essential, especially in regions identified as highly susceptible. Continuous data collection can provide early warning and assist in disaster preparedness.

Mitigation Measures: Based on the susceptibility maps, targeted mitigation measures should be implemented in high-risk areas. These may include engineering solutions, land use planning, and infrastructure improvements to reduce the impact of landslides.

Public Awareness: Raise awareness of landslide risks and safety measures among local communities and stakeholders. Effective communication can play a crucial role in reducing the vulnerability of communities to landslides.

Further Research: Expand the scope of research by considering additional factors or incorporating dynamic variables such as climate change. Investigate the potential impact of urbanization and land use changes on landslide susceptibility.

Outlook perspectives

Looking ahead, future research can explore advanced modeling techniques and incorporate real-time data sources such as remote sensing and weather forecasts to improve the accuracy of landslide susceptibility predictions. Moreover, extending the geographical scope to neighboring regions and evaluating the transferability of the models would contribute to a broader understanding of landslide dynamics in North Africa.

Additionally, the integration of risk assessment models with emergency response systems can facilitate rapid and effective responses to landslide events, potentially saving lives and reducing property damage. Collaborative efforts among researchers, government agencies, and local communities will be pivotal in developing comprehensive strategies for landslide risk reduction and sustainable land management in the region.

References

Achour Y., Boumezbeur A., Hadji R. 2017. Landslide susceptibility mapping using analytic hierarchy process and information value methods along a highway road section in Constantine, Algeria. Arab. J. Geosci., 10, 194.

Asmoay A.A., Mabrouk W.A. 2023. Appraisal of rock–water interaction and frailty of groundwater to corrosion and salinization, northwestern Gulf of Suez, Egypt. Journal of Umm Al-Qura University for Applied Sciences, 1–12.

Bagwan W.A., Gavali R.S., Maity A. 2023. Quantifying soil organic carbon (SOC) density and stock in the Urmodi River watershed of Maharashtra, India: implications for sustainable land management. Journal of Umm Al-Qura University for Applied Sciences, 1–17.

Boubazine L., Boumazbeur A., Hadji R., Fares K. 2022. Mining of Mineral Deposits.

Brahmi S., Baali F., Hadji R., Brahmi S., Hamad A., Rahal O., ... Hamed Y. 2021. Assessment of groundwater and soil pollution by leachate using electrical resistivity and induced polarization imaging survey. Case of Tebessa municipal landfill, NE Algeria. Arabian Journal of Geosciences, 14(4), 1–13.

Conforti M., Aucelli P.P., Robustelli G., Scarciglia F. 2011. Geomorphology and GIS analysis for mapping gully erosion susceptibility in the Turbolo stream catchment (Northern Calabria, Italy). Natural Hazards, 56, 881–898.

Dahal R.K., Hasegawa S., Nonomura A., Yamanaka M., Masuda T., Nishino K. 2008. GIS-based weights-of-evidence modelling of rainfall-induced landslides in small catchments for landslide susceptibility mapping. Environmental Geology, 54, 311–324.

Dahoua L., Savenko VY., Hadji R. 2017b. GIS-based technic for roadside-slope stability assessment: an bivariate approach for A1 East-west highway, North Algeria. Mining Science, 24, 81–91.

Dahoua L., Usychenko O., Savenko V.Y., Hadji R. 2018. Mathematical approach for estimating the stability of geotextile-reinforced embankments during an earthquake. Mining Science, 25, 207–217.

Dahoua L., Yakovitch S.V., Hadji R., Farid Z. 2017a. Landslide Susceptibility Mapping Using Analytic Hierarchy Process Method in BBA – Bouira Region. Case Study of East-West Highway, NE Algeria. In: Recent Advances in Environmental Science from the Euro-Mediterranean and Surrounding Regions. Eds. A. Kallel, M. Ksibi, H. Ben Dhia, N. Khélifi. EMCEI 2017. Advances in Science, Technology & Innovation (IEREK Interdisciplinary Series for Sustainable Development). Springer, Cham.

Dib I., Khedidja A., Chattah W., Hadji R. 2022. Multivariate statistical-based approach to the physical-chemical behavior of shallow groundwater in a semiarid dry climate. The case study of the Gadaïne-Ain Yaghout plain NE Algeria. Mining of Mineral Deposits, 16(3), 38-47. https://doi.org/10.33271/mining16.03.038

El Hafyani M., Essahlaoui N., Essahlaoui A., Mohajane M., Van Rompaey A. 2023. Generation of climate change scenarios for rainfall and temperature using SDSM in a Mediterranean environment: a case study of Boufakrane river watershed, Morocco. Journal of Umm Al-Qura University for Applied Sciences, 1–13.

Foumelis M., Lekkas E., Parcharidis I. 2004. Landslide susceptibility mapping by GIS-based qualitative weighting procedure in Corinth area. Bull. Geol. Soc., Greece, XXXVI, 904–912.

Fredj M., Hafsaoui A., Riheb H., Boukarm R., Saadoun A. 2020. Back-analysis study on slope instability in an open pit mine (Algeria). Scientific Bulletin of National Mining University, 2.

Kallel A., Ksibi M., Dhia H.B., Khélifi N. (eds.). 2018. Recent advances in environmental science from the Euro-Mediterranean and surrounding regions. Proceedings of Euro-Mediterranean Conference for Environmental Integration (EMCEI-1), Tunisia 2017. Springer International Publishing.

Karim Z., Hadji R., Hamed Y. 2019. GIS-based approaches for the landslide susceptibility prediction in Setif Region (NE Algeria). Geotechnical and Geological Engineering, 37(1), 359–374.

Kerbati N.R., Gadri L., Hadji R. et al. 2020. Graphical and Numerical Methods for Stability Analysis in Surrounding Rock of Underground Excavations. Example of Boukhadra Iron Mine NE Algeria. Geotechnical and Geological Engineering, 1–9.

Lee S., Pradhan B. 2007. Landslide hazard mapping at Selangor, Malaysia using frequency ratio and logistic regression models. Landslides, 4, 33–41.

Lee S., Sambath T. 2006. Landslide susceptibility mapping in the Damrei Romel area, Cambodia using frequency ratio and logistic regression models. Environ. Geol., 50(6), 847–855.

Mahdadi F., Boumezbeur A., Hadji R., Kanungo D.P., Zahri F. 2018. GIS-based landslide susceptibility assessment using statistical models: A case study from Souk Ahras province, NE Algeria. Arabian Journal of Geosciences, 11(17), 476.

Mahleb A., Hadji R., Zahri F., Boudjellal R., Chibani A., Hamed Y. 2022. Water-Borne Erosion Estimation Using the Revised Universal Soil Loss Equation (RUSLE) Model Over a Semiarid Watershed: Case Study of Meskiana Catchment, Algerian-Tunisian Border. Geotechnical and Geological Engineering, 40(8), 4217–4230.

Manchar N., Benabbas C., Hadji R., Bouaicha F., Grecu F. 2018. Landslide Susceptibility Assessment in Constantine Region Algeria by Means of Statistical Models. Studia Geotechnica et Mechanica, 40(3), 208–219.

Merghadi A., Yunus A.P., Dou J., Whiteley J., Thai Pham B., Bui D.T., ... Abderrahmane B. 2020. Machine learning methods for landslide susceptibility studies: A comparative overview of algorithm performance. Earth-Science Reviews, 207, 103225.

Nekkoub A., Baali F., Hadji R., Hamed Y. 2020. The EPIK multi-attribute method for intrinsic vulnerability assessment of karstic aquifer under semi-arid climatic conditions, case of Cheria Plateau, NE Algeria. Arabian Journal of Geosciences, 13(15), 1–15.

Neuhäuser B., Terhorst B. 2007. Landslide susceptibility assessment using B weights-of evidence applied to a study area at the Jurassic escarpment (SW Germany). Geomorphology, 86(1), 12–24.

Orabi O.H., El-Sabbagh A., Mansour A.S., Ismail H., Taha S. 2023a. Foraminifera study for the characterization of the Campanian/Maastrichtian boundary in Gebel Owaina, Nile Valley, Egypt. Journal of Umm Al-Qura University for Applied Sciences, 1–19.

Orabi O.H., Hamad M.M., Abu Saima M.M. 2023b. Foraminifera dissolution phases in the upper cretaceous succession of Jebel Duwi, Egypt. Journal of Umm Al-Qura University for Applied Sciences, 1–19.

Pourghasemi H.R., Moradi H.R., Fatemi Aghda S.M. 2013. Landslide susceptibility mapping by binary logistic regression, analytical hierarchy process, and statistical index models and assessment of their performances. Nat Hazards, 69, 749–779.

Pourghasemi H.R., Pradhan B., Gokceoglu C. 2012. Application of fuzzy logic and analytical hierarchy process (AHP) to landslide susceptibility mapping at Haraz watershed, Iran.

Raïs K., Kara M., Gadri L., Hadji R., Khochman L. 2017. Original approach for the drilling process optimization in open cast mines: case study of Kef Essenoun open pit mine Northeast of Algeria. Mining Science, 24, 147–159.

Saaty T.L. 1980. The analytical hierarchy process. McGraw Hill, New York.

Saaty T.L. 2000. The fundamentals of decision making and priority theory with the analytic hierarchy process, VI, 2nd ed. RWS Publications, Pitsburg.

Saha A.K., Gupta R.P., Sarkar I., Arora M.K., Csaplovics E. 2005. An approach for GIS-based statistical landslide susceptibility zonation with a case study in the Himalayas. Landslides, 2, 61–69.

Sánchez-García V., Mateos R.M. 2020. Assessment of natural hazards and risk in Mediterranean countries. Sustainability, 12(10), 4217.

Sankar T.K., Ambade B., Mahato D.K., Kumar A., Jangde R. 2023. Anthropogenic fine aerosol and black carbon distribution over urban environment. Journal of Umm Al-Qura University for Applied Sciences, 1–10.

Taib H., Hadji R., Hamed Y., Bensalem M.S., Amamria S. 2023. Exploring neotectonic activity in a semiarid basin: a case study of the Ain Zerga watershed. Journal of Umm Al-Qura University for Applied Sciences, 1–14.

Van Westen C.J., Rengers N., Soeters R. 2003. Use of geomorphological information in indirect landslide susceptibility assessment. Nat Hazards, 30(3), 399–419.

Wang Q., Guo Y., Li W., He J., Wu Z. 2019. Predictive modeling of landslide hazards in Wen County, northwestern China based on information value, weights-of-evidence, and certainty factor. Geomatics, Natural Hazards and Risk, 10(1), 820–835.

Yilmaz C., Topal T., Suzen M.L. 2012. GIS-based landslide susceptibility mapping using bivariate statistical analysis in Devrek (Zonguldak, Turkey). Environ. Earth Sci., 65, 2161–2178.

Post-doctoral degree Rania Boudjellal
Department of Earth and Universe Sciences
Laboratory of Water and Environment
Faculty of Exact Sciences and Natural and Life Sciences
Echahid Larbi Tebessi University, Algeria
e-mail: eng.geol.dz@gmail.com

Prof. Chemseddine Fehdi
Department of Earth and Universe Sciences
Laboratory of Water and Environment
Faculty of Exact Sciences and Natural and Life Sciences
Echahid Larbi Tebessi University, Algeria
e-mail: fehdi@yahoo.fr

Prof. Fethi Baali
Department of Earth and Universe Sciences
Laboratory of Water and Environment
Faculty of Exact Sciences and Natural and Life Sciences
Echahid Larbi Tebessi University, Algeria
e-mail: baali_fr2000@yahoo.fr